# Development of a Real-time RT-PCR Assay for Detecting EGFRvIII in Glioblastoma Samples

Koji Yoshimoto,[1] Julie Dang,[1] Shaojun Zhu,[1] David Nathanson,[1,2] Tiffany Huang,[1] Rebecca Dumont,[1] David B. Seligson,[1] William H. Yong,[1] Zhenggang Xiong,[1] Nagesh Rao,[1] Henrik Winther,[8] Arnab Chakravarti,[9] Darell D. Bigner,[10] Ingo K. Mellinghoff,[2,6,7] Steve Horvath,[3,4] Webster K. Cavenee,[11] Timothy F. Cloughesy,[5,6,7] and Paul S. Mischel[1,2,5,6,7]

**Abstract**

**Purpose:** Epidermal growth factor receptor variant III (*EGFRvIII*) is an oncogenic, constitutively active mutant form of the *EGFR* that is commonly expressed in glioblastoma and is also detected in a number of epithelial cancers. EGFRvIII presents a unique antigenic target for anti-EGFRvIII vaccines and it has been shown to modulate response to EGFR kinase inhibitor therapy. Thus, detection in clinical samples may be warranted. Existing patents preclude the use of anti-EGFRvIII antibodies for clinical detection. Further, frozen tissue is not routinely available, particularly for patients treated in the community. Thus, detection of EGFRvIII in formalin-fixed paraffin-embedded (FFPE) clinical samples is a major challenge.

**Experimental Design:** We developed a real-time reverse transcription-PCR (RT-PCR) assay for detecting *EGFRvIII* in FFPE samples and analyzed 59 FFPE glioblastoma clinical samples with paired frozen tissue from the same surgical resection. We assessed EGFRvIII protein expression by immunohistochemistry using two distinct specific anti-EGFRvIII antibodies and examined *EGFR* gene amplification by fluorescence *in situ* hybridization.

**Results:** The FFPE RT-PCR assay detected *EGFRvIII* in 16 of 59 (27%) samples, exclusively in cases with *EGFR* amplification, consistent with the expected frequency of this alteration. The FFPE RT-PCR assay was more sensitive and specific for detecting EGFRvIII than either of the two antibodies alone, or in combination, with a sensitivity of 93% (95% confidence interval, 0.78-1.00) and a specificity of 98% (95% confidence interval, 0.93-1.00).

**Conclusion:** This assay will facilitate accurate assessment of *EGFRvIII* in clinical samples and may aid in the development of strategies for stratifying patients for *EGFRvIII*-directed therapies.

Molecularly targeted therapies promise to transform the treatment of cancer patients, including those with glioblastoma, the most common malignant primary brain tumor of adults. The epidermal growth factor receptor (*EGFR*) is a compelling molecular target in glioblastoma because it is amplified, overexpressed, and/or mutated in up to 40% to 50% of patients (1–4). *EGFRvIII*, the most common glioblastoma *EGFR* mutation in glioblastoma, results from an in-frame deletion of 801 bp spanning exons 2 to 7 of the coding region of *EGFR* (4–6). This leads to ligand-independent tyrosine kinase activity that activates persistent downstream phosphatidylinositol 3′-kinase pathway activation and promotes tumor

**Authors' Affiliations:** Departments of [1]Pathology and Laboratory Medicine, [2]Molecular and Medical Pharmacology, [3]Human Genetics, [4]Biostatistics, and [5]Neurology, [6]Jonsson Comprehensive Cancer Center, and [7]Henry E. Singleton Brain Tumor Program, David Geffen School of Medicine, University of California at Los Angeles, Los Angeles, California; [8]DAKO A/S, Glostrup, Denmark; [9]Department of Radiation Oncology, Massachusetts General Hospital/Harvard Medical School, Boston, Massachusetts; [10]Department of Pathology and The Preston Robert Tisch Brain Tumor Center at Duke, Durham, North Carolina; and [11]Ludwig Institute for Cancer Research at University of California, La Jolla, San Diego, California

Received 8/9/07; revised 9/28/07; accepted 10/10/07.

**Grant support:** Brain Tumor Funders' Collaborative; National Institute for Neurological Disorders and Stroke grant NS050151 (P.S. Mischel); National Cancer Institute grants CA108633 (A. Chakravarti and P.S. Mischel), CA119347 (P.S. Mischel), and CA95616 (W.K. Cavenee); Fellow Award from the National Foundation for Cancer Research (W.K. Cavenee); Young Investigator Award from the American Society of Clinical Oncology (I.K. Mellinghoff). This work was also supported by the Harry Allgauer Foundation through The Doris R. Ullmann Fund for Brain Tumor Research Technologies, the Henry E. Singleton Brain Tumor Foundation, the Phase One Foundation, a generous donation from the Ziering Family Foundation in memory of Sigi Ziering, Art of the Brain and the Roven Family Fund in memory of Dawn Steel. T. Huang received a training grant from the University of California at Los Angeles Scholars in Oncologic Imaging Training Program. R. Dumont received support through a Howard Hughes Medical Student Training Fellowship.

The costs of publication of this article were defrayed in part by the payment of page charges. This article must therefore be hereby marked *advertisement* in accordance with 18 U.S.C. Section 1734 solely to indicate this fact.

**Note:** Supplementary data for this article are available at Clinical Cancer Research Online (http://clincancerres.aacrjournals.org/).

Current address for K. Yoshimoto: Department of Neurosurgery, Graduate School of Medical Sciences, Kyushu University, Fukuoka, Japan.

**Requests for reprints:** Paul S. Mischel, Department of Pathology and Laboratory Medicine, David Geffen School of Medicine, University of California at Los Angeles, 10833 Le Conte, Los Angeles, CA 90095-1732. Phone: 310-825-0377; Fax: 310-206-8290; E-mail: pmischel@mednet.ucla.edu.



doi:10.1158/1078-0432.CCR-07-1966

growth (4, 7, 8). *EGFRvIII* occurs in up to 20% to 30% of glioblastoma patients (9) and has also been reported in a number of epithelial cancers (10–16).

We recently showed that EGFRvIII expression is associated with favorable clinical response to the EGFR kinase inhibitors gefitinib and erlotinib in glioblastoma patients whose tumors have retained the phosphatase and tensin homologue tumor suppressor protein (17). This observation has been confirmed both *in vitro* and in patient-derived xenografts (18). Thus, EGFRvIII may potentially be useful for identifying patients who may respond to EGFR kinase inhibitor therapy. EGFRvIII also presents a unique antigenic target on tumor cells. This property is currently being therapeutically exploited with anti-EGFRvIII vaccines, including one which has shown promise in an early phase II clinical trials (16, 19). Such molecularly targeted approaches have made clinical detection of EGFRvIII a priority.

Currently, detection of EGFRvIII in clinical samples presents a significant challenge. Immunohistochemical detection using EGFRvIII specific antibodies has been shown (20, 21). However, existing patents prohibit the use of any antibody that recognizes the unique antigenic structure of EGFRvIII for clinical detection. Thus, widespread clinical testing for EGFRvIII by immunohistochemistry is not possible. Reverse transcription-PCR (RT-PCR) and Southern blot assays have been developed for detection of *EGFRvIII* in frozen tissue (9). Frozen tissue is not routinely available, particularly in patients treated in the community. Thus, approaches for EGFRvIII detection in routinely processed formalin-fixed paraffin-embedded (FFPE) tissue samples are lacking. Here, we report the development of a highly sensitive and specific RT-PCR assay for *EGFRvIII* mRNA detection in routinely processed FFPE clinical glioblastoma samples.

## Materials and Methods

***Tumor samples.*** All paraffin blocks and frozen tissues were collected from the patients who underwent surgery at the University of California at Los Angeles Medical Center. A total of 59 paraffin tissue blocks, 54 of which have corresponding frozen tissues available, were used for this study. All specimens were obtained according to a protocol approved by the institutional review board of University of California at Los Angeles. All tumors were diagnosed as glioblastoma (WHO grade 4) according to WHO grading system. Tumor tissues were incubated in 10% neutral-buffered formalin after surgical removal and paraffin embedded. For frozen tissues, tumor tissues were snap frozen in liquid nitrogen and stored at -80°C until they were processed.

***RNA extraction from tumor tissues.*** Paraffin tumor blocks were cut into 10-μm slices and 5 to 10 slices of tissue were put into 1.5-mL microtubes. The tissues were deparaffinized by xylene and ethanol. Total RNA from paraffin-embedded tissues was extracted using Optimun FFPE RNA Isolation Kit (Ambion Diagnostics) or hybrid method with Trizol (Invitrogen). In hybrid method, total RNA was extracted by Trizol after proteinase K treatment and dissolved in 100 μL of RNase-free water, which was further purified using Optimun FFPE RNA Isolation Kit according to the manufacturer's protocol. All RNA samples were rigorously treated with DNase and confirmed to be not amplified by HPRT1 genomic PCR primers within 35 PCR cycles, which showed that residual DNA in these samples is of minimum quantity. Concentration of the extracted RNA was quantified by SmartSpec 3000 spectrophotometer (Bio-Rad) or NanoDrop ND-3300 fluorospectrometer (NanoDrop). Average RNA yield was 2 to 5 μg and absorbance ratio of 260/280 nm was >1.8 in most of the samples. RNA quality was assessed using Agilent 2100 Bioanalyzer with RNA LabChip kit (Agilent) for some samples. RNA from the frozen tissues was extracted using Trizol (Invitrogen) according to the manufacturer's protocol and quantified.

***Real-time RT-PCR.*** Reverse transcription was done using Superscipt II Transcriptase (Invitrogen) according to the manufacturer's protocol. To examine the quantitative feature of this assay, the following strategy was taken. For paraffin tissue–derived RNA, 75, 150, and 300 ng of RNA were used as template of reverse transcription reactions in each sample. For frozen tissue–derived RNA, 150, 300, and 600 ng were used as template. Reverse transcription reaction was done in a total volume of 20 μL including RNA template, 200 mmol/L gene-specific primers, reverse transcription buffer, 5 mmol/L $MgCl_2$, 10 mmol/L DTT, RNase inhibitor, and 50 units of SuperScript II reverse transcriptase. All the samples were treated by RNase H after reverse transcription.

We designed two kinds of *EGFRvIII*-specific primers (Supplementary Table S1) to amplify *EGFRvIII*, one of which was used for real-time analysis (*EGFRvIII-2*). *HPRT1* and *GUSB* were used as control genes and PCR primer information was derived from the previous reports and synthesized. Control reactions were prepared in parallel without reverse transcriptase with 300 ng of RNA extracted from paraffin and 600 ng of RNA from frozen tissues. In total, four reactions were done for each sample.

Real-time PCR was done on iCycler (Bio-Rad) using SYBR green method. Two microliters of cDNA product were used as a template in a 25-μL PCR reaction containing 12.5 μL of SYBR mixture (iQTM SYBR Green Supermix, Bio-Rad), 200 mmol/L of each primer, 1.25 μL of DMSO, and 8.25 μL of distilled water. All reactions were done in duplicate. Amplification protocols were followed: 95°C for 3 min; 40 cycles of 95°C/10 s, 60°C/30 s, and 72°C/30 s; and 80 cycles of 55 + 0.5°C per cycle for melting curve analysis. Threshold cycle number (Ct) was automatically determined by iQ software (Bio-Rad).

***Data analysis of real-time PCR.*** Mean Ct number of duplicate run was used for data analysis. The reference gene Ct number was determined by averaging the number of two reference genes (*GUSB* and *HPRT1*). The relative expression of *EGFRvIII* compared with reference gene was calculated as ΔCt (Δthreshold cycle), which was calculated by subtracting the Ct number of reference gene from that of *EGFRvIII*.

***Conventional RT-PCR.*** Conventional RT-PCR using *EGFRvIII*-specific primer 1 was done for 300 ng of paraffin RNA with no transcriptase control. PCR was done in a 20-μL reaction containing 2 μL of cDNA, 200 mmol/L of primer, 200 μmol/L nucleotide, 1.5 mmol/L $MgCl_2$, 5% DMSO, and 2 units of Platinum Taq polymerase (Invitrogen). PCR cycling conditions began with initial denaturation step at 94°C for 2 min, followed by 35 cycles of 94°C denaturation for 30 s, 60°C annealing for 30 s, and 72°C extension for 1 min. Conventional RT-PCR using common primers that amplify wild-type and EGFRvIII from frozen RNA was done according to previously described methods (17).

***Genomic PCR and sequencing.*** Genomic DNA from *EGFRvIII*-positive samples was used for long-range PCR to make sure the genomic deletion within intron 1 and intron 7. PCR primers and sequence primers were synthesized from the previous report with some modifications (4). Long-range PCR was done using Platinum Taq High Fidelity DNA polymerase (Invitrogen) with 100 to 200 ng of genomic DNA according to the manufacturer's protocol. PCR cycling condition began with an initial denaturation step at 94°C for 1 min, followed by 14 cycles of 98°C denaturation for 10 s, 68°C extension for 15 min with extension by 15 s each cycle after the 15th cycle, and final extension for 10 min at 68°C. PCR products were visualized by 0.8% agarose gel eletrophoresis and the breakpoint was confirmed by direct sequencing.

***Immunohistochemistry and image analysis–based scoring.*** Sections were stained with clone L8A4 (a generous gift from Dr. Darell Bigner) and DAK-H1-VIII. The specificity of the L8A4 antibody has previously been well described (13). The DAK-H1-VIII antibody was raised against

a peptide that covers the junction between amino acids 25 (L)→29 (K) and 298 (N)→307 (C). The 17-mer peptide amino acid sequence n-LEEKK-NYVVTDHGSC-c- was conjugated to a purified protein derivative carrier. The specificity of DAK-H1-VIII is shown in Fig. 2.

Immunohistochemistry for L8A4 and DAK-H1-VIII was done according to the same protocol previously described (17). Briefly, antigen retrieval was done using 0.01 mol/L citrate buffer (pH 6) in pressure cooker for 10 min. Peroxidase activity was quenched with 3% hydrogen peroxide in water. Primary antibodies (L8A4 at 1:150, DAK-H1-VIII at 1:100) were diluted in PBS with 2% bovine horse serum and applied for 1 h at room temperature, followed by M-polymer horseradish peroxidase reactions for 20 min at room temperature. Vector NovaRed was used as the enzyme substrate to visualize specific antibody localization. Slides were counterstained with Harris hematoxylin. Representative images from EGFRvIII immunostained sections with L8A4 were photographed using a Colorview II camera mounted on an Olympus BX61 microscope. Multiple images were captured (at least three per slide) from representative regions of the tumor and adjacent normal brain if present. Borders between individual cells were approximated using a filter function. The amount of reaction product per cell was determined by measuring mean saturation per cell in the red-brown hue range. As an internal control, mean saturation was measured in adjacent normal brain tissue. For samples in which no adjacent normal brain was present on the slide, a normal reference standard was established. Cutoff value for positive staining is 1.5 as previously described (17).

***Fluorescence* in situ *hybridization.*** Dual probe fluorescence *in situ* hybridization was done on paraffin-embedded sections with locus-specific probes for EGFR and centromere of chromosome 7 (CEP7; Vysis, Downers Grove, IL).

## Results

We developed a two step RT-PCR using junction-specific primers that recognize the specific sequences created by the in-frame genomic deletion within exons 2 to 7 of *EGFRvIII* (Supplementary Table S1; Fig. 1A; see Supplementary methods for complete assay details). This results in amplification of a single band detected by conventional semiquantitative RT-PCR (Fig. 1B). Direct sequencing confirmed amplification of *EGFRvIII* (Fig. 1C). Incorporation of these primers into a fluorogenic real-time RT-PCR assay using *GUSB* and *HPRT1* as control genes showed striking linearity for *EGFRvIII* detection (Fig. 1D).

We used the RT-PCR assay (both conventional and real-time) to detect *EGFRvIII* in a series of FFPE glioblastoma clinical samples ($n$ = 59). In parallel, EGFRvIII protein was assessed by immunohistochemistry using two distinct and specific anti-EGFRvIII antibodies, the mouse monoclonal L8A4 antibody (22) and a newly generated mouse monocloncal anti-EGFRvIII



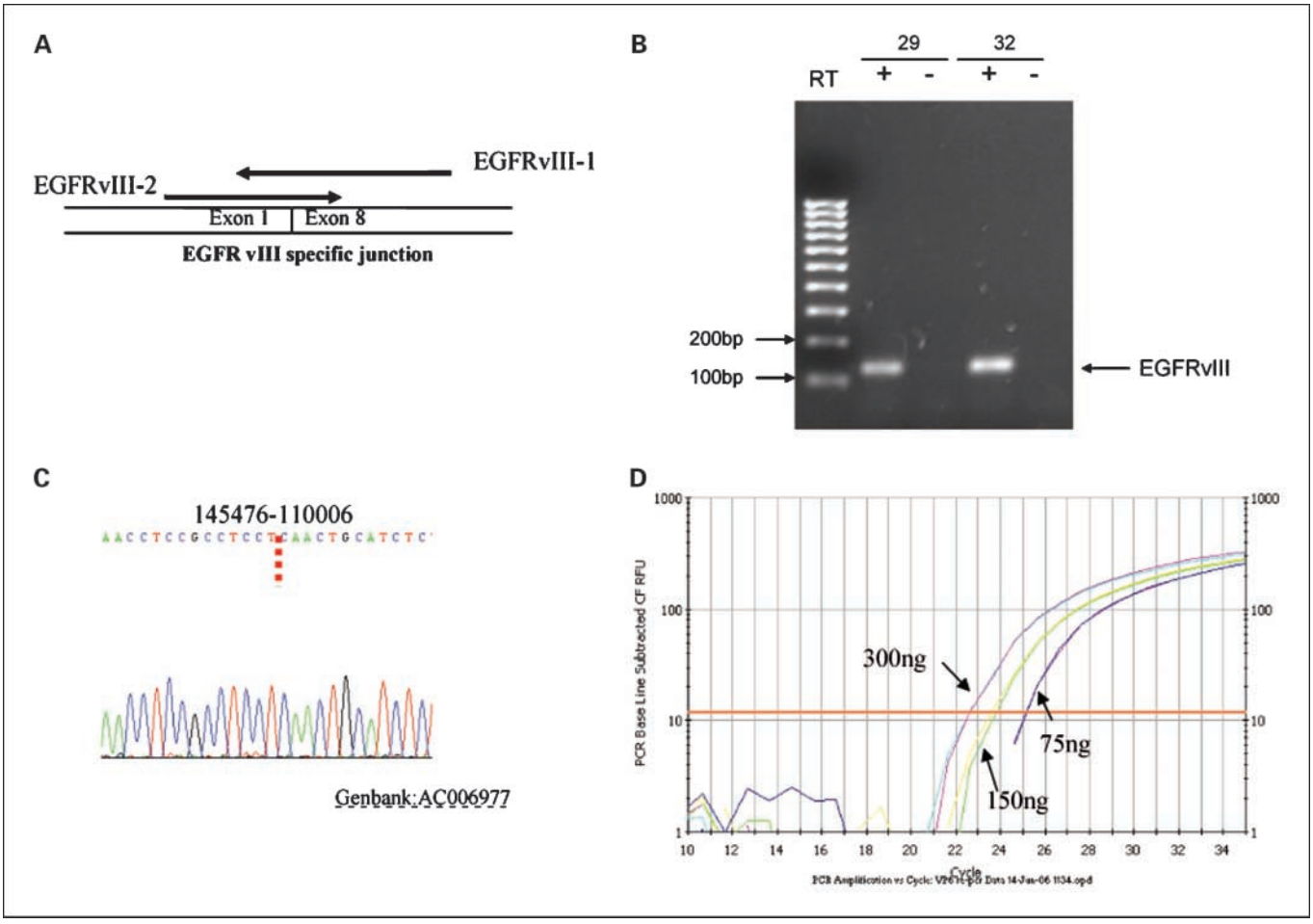


**Fig. 1.** RT-PCR strategy for detection of EGFRvIII. *A*, schematic depiction of the annealing sites for reverse primer of the specific primer 1 and forward primer of the specific primer 2. *B*, agarose gel images of conventional semiquantitative RT-PCR (samples 29 and 32) with and without reverse transcriptase. *C*, direct sequencing of the genomic DNA fragment amplified by long-range genomic PCR shows the genomic deletion in intron 1 (*110006 nt*) and intron 7 (*145476 nt*) and confirms the presence of EGFRvIII. *D*, real-time RT-PCR showing quantitative detection of EGFRvIII depending on the starting RNA dose (75, 150, and 300 ng).

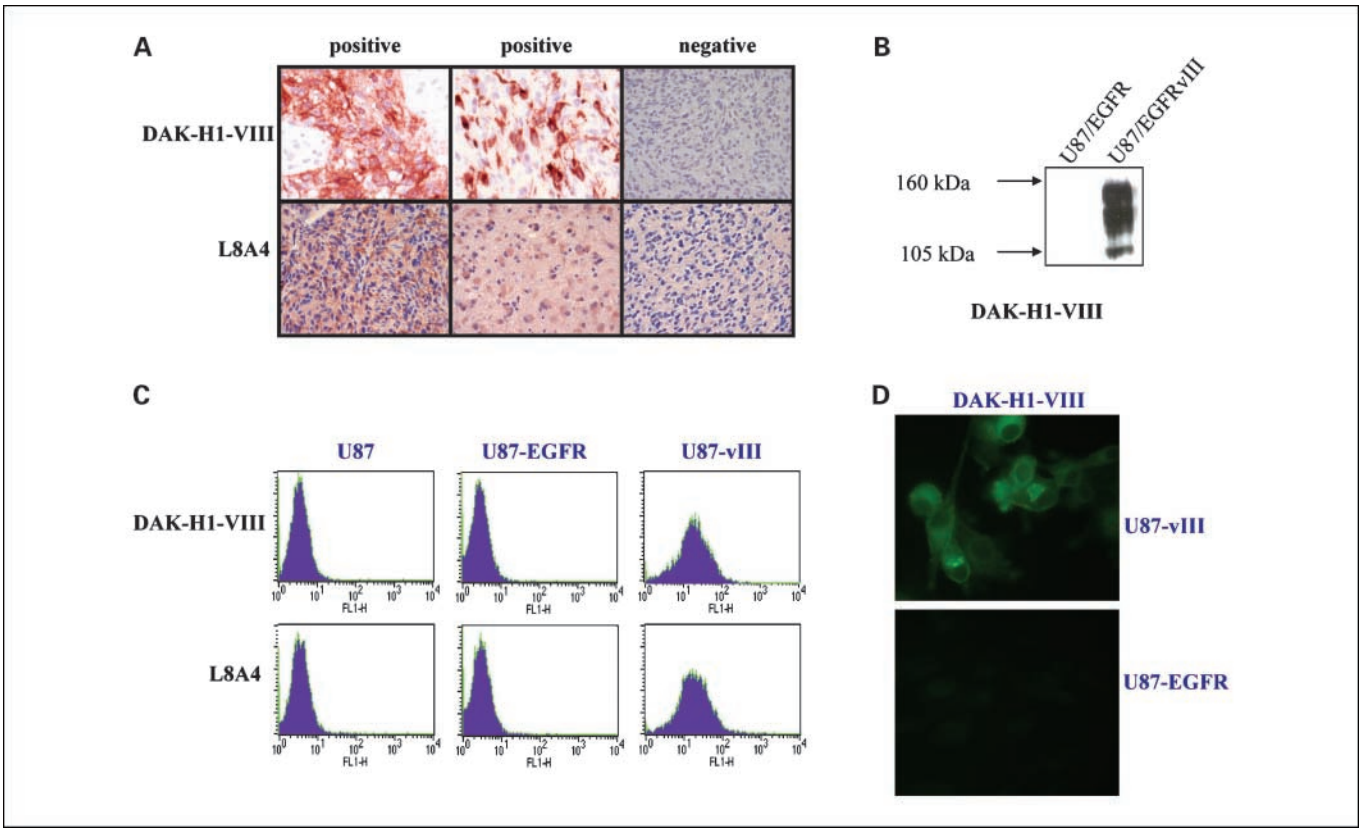


**Fig. 2.** Immunohistochemical detection of EGFRvIII. *A*, representative images of EGFRvIII-positive and EGFRvIII-negative samples with DAK-H1-VIII and L8A4 antibodies. *B*, biochemical immunoblot analysis of DAK-H1-VIII revealed specific detection of EGFRvIII. *C*, flow cytometry showed that DAK-H1-VIII and L8A4 detected only cell-surface EGFRvIII expression. *D*, immunocytochemical staining showed specific recognition of EGFRvIII and not wild-type EGFR.

antibody raised against a junction-specific peptide (DAK-H1-vIII). Both antibodies specifically recognize EGFRvIII, but not wild-type EGFR, as shown in biochemical and immunocytochemical assays (Fig. 2B and D). Both antibodies also detect cell-surface EGFRvIII expression (Fig. 2C). EGFRvIII immunohistochemistry was analyzed using both semiquantitative and quantitative automated image analysis, as previously described (17). We also assessed *EGFR* gene amplification by fluorescence *in situ* hybridization, and we assessed *EGFRvIII* mRNA expression by RT-PCR in the paired frozen tissue, which was available in 54 of 59 cases. Complete data for all of these assays are presented in Supplementary Table S2.

*EGFRvIII* was detected by RT-PCR in 16 of 59 (27%) of the FFPE samples, consistent with the expected frequency of this alteration (4, 9). The conventional semiquantitative and real-time fluorogenic RT-PCR assays showed 100% concordance [$\kappa$ = 1.0; 95% confidence interval (95% CI), 1.0-1.0]. *EGFRvIII* was also detected exclusively in cases with *EGFR* amplification, consistent with previous findings. Immunohistochemical analysis of these samples showed EGFRvIII in 20 of 59 (34%) with the L8A4 antibody and in 15 of 59 (25%) with DAK-H1-vIII (Supplementary Table S2). The FFPE RT-PCR assay showed very good agreement with both the L8A4 and DAK-H1-vIII antibodies [L8A4, $\kappa$ = 0.80 (95% CI, 0.63-0.81); DAK-H1-vIII, $\kappa$ = 0.82 (95% CI, 0.64-1.00); Table 1]. This was superior to the agreement between the L8A4 and DAK-H1-vIII antibodies ($\kappa$ = 0.62; 95% CI, 0.40-0.85). A composite antibody biomarker (positive only if both L8A4 and DAK-H1-vIII are positive) showed an even better agreement with the FFPE RT-PCR result ($\kappa$ = 0.91; 95% CI, 0.78-1.00). Of the paraffin detection methods, the RT-PCR assay was the most correlated with the frozen tissue RT-PCR ($r$ = 0.76; $P = 3.7 \times 10^{-11}$). Immunohistochemical detection with either antibody showed significantly lower correlation with the frozen tissue RT-PCR (L8A4 antibody: $r$ = 0.61; $P = 1.4 \times 10^{-6}$; DAK-H1-vIII antibody: $r$ = 0.55; $P = 3 \times 10^{-5}$). The composite antibody biomarker (positive only if both L8A4 and DAKO were positive) improved the correlation with the frozen tissue RT-PCR ($r$ = 0.66; $P = 4.4 \times 10^{-8}$), but not to the level of the paraffin RT-PCR. Adding the combination antibody biomarker to the RT-PCR assay also did not improve correlation with the frozen tissue RT-PCR assay. Thus, the real-time RT-PCR assay on FFPE tissue showed the best correlation with RT-PCR detection.

The RT-PCR assay on frozen tissue yielded three kinds of signals: strong positives (6 of 54; 11%), clear negatives (35 of 53; 65%), and 13 cases with a weak signal (24%). All six of the samples that showed strong *EGFRvIII* mRNA expression on frozen tissue were positive for *EGFRvIII* in the FFPE RT-PCR assay. Similarly, 33 of 35 (94%) *EGFRvIII*-negative samples on frozen tissue showed no evidence of *EGFRvIII* mRNA in the FFPE RT-PCR assay. Thus, the FFPE RT-PCR assay was highly sensitive (100%) and specific (94%) for detecting *EGFRvIII* in cases where the RT-PCR from frozen tissue yielded an unequivocal result. Next, we assessed the RT-PCR and immunohistochemistry results on the FFPE samples for which the paired frozen tissue yielded a weak *EGFRvIII* signal. We

**Table 1.** Statistical comparison at EGFRvIII detection methods

**Correlations of FFPE samples**

| Comparison | κ (95% CI) |
|---|---|
| L8A4 vs DAK-vIII | 0.62 (0.40-0.85) |
| FFPE RT-PCR* | 0.80 (0.63-0.81) |
| FFPE RT-PCR vs DAK-vIII | 0.82 (0.64-1.00) |
| FFPE RT-PCR vs L8A4 + DAK-vIII | 0.91 (0.78-1.00) |

**Correlations between FFPE and frozen samples**

| Comparison | *r* (*P*) |
|---|---|
| Frozen tissue RT-PCR vs L8A4 | 0.6 ($1.4 \times 10^{-6}$) |
| Frozen tissue RT-PCR vs DAK-vIII | 0.55 ($3.0 \times 10^{-5}$) |
| Frozen tissue RT-PCR vs L8A4 + DAK-vIII | 0.66 ($4.4 \times 10^{-8}$) |
| Frozen tissue RT-PCR vs FFPE RT-PCR* | 0.76 ($3.7 \times 10^{-11}$) |

**Clinical utility** †

| Measure | % (95% CI) |
|---|---|
| Sensitivity | 93 (78-100) |
| Specificity | 98 (93-100) |
| Positive predictive value | 93 (78-100) |
| Negative predictive value | 98 (93-100) |

*FFPE RT-PCR showed identical findings using either conventional semiquantitative detection on agarose gels or quantitative detection in the real-time RT-PCR assay.
† True-positive cases consist of samples that are EGFRvIII positive on frozen tissue RT-PCR and are positive on FFPE tissue with L8A4 + DAK-vIII antibodies.

reasoned that this weak signal could be due to heterogeneous expression of *EGFRvIII* mRNA and protein within a limited number of tumor cells within the biopsy. Alternatively, the low-level mRNA expression might not be sufficient to generate detectable amounts of EGFRvIII protein. The FFPE RT-PCR detected *EGFRvIII* mRNA in 6 of 6 cases with weak signal on frozen tissue but positive EGFRvIII protein detection using both antibodies for immunohistochemistry. In contrast, the FFPE RT-PCR did not detect *EGFRvIII* in 6 of 7 cases in which a weak signal was seen on frozen tissue but no EGFRvIII was detected with either antibody ($P = 0.0047$, Fisher's exact test). Thus, the FFPE RT-PCR assay distinguished between samples that did or did not express EGFRvIII protein, providing an accurate and unambiguous readout of EGFRvIII that correlates with protein expression in routinely processed clinical samples.

To assess the sensitivity and specificity of this assay, we defined a stringent consensus gold standard. We considered all cases with detectable *EGFRvIII* mRNA by RT-PCR on frozen tissue and EGFRvIII protein immunopositivity by both antibodies in matched paraffin samples as true positives. We adopted this gold standard because we have previously shown its association with a clinical outcome (i.e. response to EGFR kinase inhibitor therapy; ref. 17). Using this approach, the RT-PCR assay from the paraffin-embedded tissue showed a sensitivity of 93% (95% CI, 0.78-1.00) and a specificity of 98% (95% CI, 0.93-1.00), with an area under the ROC of 0.95 (Table 1).

## Discussion

The development of molecularly targeted therapies has the potential to transform the care of cancer patients (17). The success of such approaches is likely to depend on developing methods to reliably detect persistently activated oncogenes and their downstream signaling networks in clinical samples (17). This is particularly true of oncogenes that can be differentially targeted with antibody-mediated therapies because of their unique antigenic structure or oncogenes that sensitize tumor cells to signal transduction inhibitors.

*EGFRvIII* is potentially a paradigmatic example of such an oncogene. It results from an in-frame genomic deletion creating a unique antigenic site that can be targeted using antibody-based vaccines, including one which has shown promise in an early phase II clinical trials (4–6, 16, 19). In addition, this mutation confers novel signal transduction properties on the receptor, including enhanced activation of the phosphatidylinositol 3′-kinase signaling pathway (20). We and others have shown that in glioblastoma patients and in cell culture and *in vivo* models, EGFRvIII sensitizes tumors to EGFR tyrosine kinase inhibitors when the tumor suppressor protein phosphatase and tensin homologue is intact (17, 18). Thus, in addition to its recently shown relevance for defining prognostically distinct subgroups (23), EGFRvIII detection is likely to be increasingly important for determining treatment decisions for patients with glioblastoma and potentially for those with other types of cancer.

A number of issues render clinical detection of EGFRvIII a serious challenge, namely, the inability to use any antibody that recognizes EGFRvIII for clinical detection in FFPE samples due to existing patents and the unavailability of frozen tissue, particularly for patients treated in the community. Thus, development of a simple, nucleic acid–based assay for definitive detection of *EGFRvIII* in FFPE samples, particularly one which can be used for clinical testing, is of significant practical value.

In summary, we have developed a highly sensitive, highly specific RT-PCR for unambiguous detection of *EGFRvIII* in routinely processed, FFPE samples. The strengths of this approach are the ease of the assay, the improved accuracy relative to the immunohistochemical tests, and the remarkable sensitivity and specificity achieved. The FFPE RT-PCR can be done either as a real-time assay, providing quantitative information, or as a semiquantitative RT-PCR for clinical laboratories that do not have access to real-time PCR equipment. This assay may facilitate widespread clinical testing for *EGFRvIII* and may be important for determining whether *EGFRvIII* is associated with response to molecularly targeted inhibitors and antitumor vaccines in patients with glioblastoma as well as in patients with other types of cancers.



## References

1. Smith JS, Tachibana I, Passe SM, et al. PTEN mutation, EGFR amplification, and outcome in patients with anaplastic astrocytoma and glioblastoma multiforme. J Natl Cancer Inst 2001;93:1246–56.
2. Ohgaki H, Kleihues P. Population-based studies on incidence, survival rates, and genetic alterations in astrocytic and oligodendroglial gliomas. J Neuropathol Exp Neurol 2005;64:479–89.
3. Heimberger AB, Hlatky R, Suki D, et al. Prognostic effect of epidermal growth factor receptor and EGFRvIII in glioblastoma multiforme patients. Clin Cancer Res 2005;11:1462–6.

4. Frederick L, Wang XY, Eley G, James CD. Diversity and frequency of epidermal growth factor receptor mutations in human glioblastomas. Cancer Res 2000; 60:1383–7.
5. Wong AJ, Ruppert JM, Bigner SH, et al. Structural alterations of the epidermal growth factor receptor gene in human gliomas. Proc Natl Acad Sci U S A 1992;89:2965–9.
6. Sugawa N, Ekstrand AJ, James CD, Collins VP. Identical splicing of aberrant epidermal growth factor receptor transcripts from amplified rearranged genes in human glioblastomas. Proc Natl Acad Sci U S A 1990;87:8602–6.
7. Tang CK, Gong XQ, Moscatello DK, et al. Epidermal growth factor receptor vIII enhances tumorigenicity in human breast cancer. Cancer Res 2000;60:3081–7.
8. Nishikawa R, Ji XD, Harmon RC, et al. A mutant epidermal growth factor receptor common in human glioma confers enhanced tumorigenicity. Proc Natl Acad Sci U S A 1994;91:7727–31.
9. Aldape KD, Ballman K, Furth A, et al. Immunohistochemical detection of EGFRvIII in high malignancy grade astrocytomas and evaluation of prognostic significance. J Neuropathol Exp Neurol 2004;63: 700–7.
10. Sok JC, Coppelli FM, Thomas SM, et al. Mutant epidermal growth factor receptor (EGFRvIII) contributes to head and neck cancer growth and resistance to EGFR targeting. Clin Cancer Res 2006;12: 5064–73.
11. Ji H, Zhao X, Yuza Y, et al. Epidermal growth factor receptor variant III mutations in lung tumorigenesis and sensitivity to tyrosine kinase inhibitors. Proc Natl Acad Sci U S A 2006;103:7817–22.
12. Li D, Ji H, Zaghlul S, et al. Therapeutic anti-EGFR antibody 806 generates responses in murine *de novo* EGFR mutant-dependent lung carcinomas. J Clin Invest 2007;117:346–52.
13. Wikstrand CJ, Hale LP, Batra SK, et al. Monoclonal antibodies against EGFRvIII are tumor specific and react with breast and lung carcinomas and malignant gliomas. Cancer Res 1995;55:3140–8.
14. Garcia de Palazzo IE, Adams GP, Sundareshan P, et al. Expression of mutated epidermal growth factor receptor by non-small cell lung carcinomas. Cancer Res 1993;53:3217–20.
15. Okamoto I, Kenyon LC, Emlet DR, et al. Expression of constitutively activated EGFRvIII in non-small cell lung cancer. Cancer Sci 2005;94:50–6.
16. Goldman B. Taming a mutinous mutant: an errant receptor becomes a prime cancer target. J Natl Cancer Inst 2007;99:504–5.
17. Mellinghoff IK, Wang MY, Vivanco I, et al. Molecular determinants of the response of glioblastomas to EGFR kinase inhibitors. N Engl J Med 2005;353: 2012–24.
18. Sarkaria, JN, Yang L, Grogan PT, et al. Identification of molecular characteristics correlated with glioblastoma sensitivity to EGFR kinase inhibition through use of an intracranial xenograft test panel. Mol Cancer Ther 2007;6:1167–74.
19. Heimberger AB, Hussain SF, Suki D, et al. An epidermal growth factor receotor variant III peptide vaccination appears promising in newly diagnosed GBM patients: preliminary results of a randomized phase II clinical trial. American Association of Neurological Surgeons; 2006.
20. Choe G, Horvath S, Cloughesy TF, et al. Analysis of the phosphatidylinositol 3′-kinase signaling pathway in glioblastoma patients *in vivo*. Cancer Res 2003;63: 2742–6.
21. McLendon RE, Wikstrand CJ, Matthews MR, et al. Glioma-associated antigen expression in oligodendroglial neoplasms. Tenascin and epidermal growth factor receptor. J Histochem Cytochem 2000;48: 1103–10.
22. Wikstrand CJ, McLendon RE, Friedman AH, Bigner DD. Cell surface localization and density of the tumor-associated variant of the epidermal growth factor receptor, EGFRvIII. Cancer Res 1997;57:4130–40.
23. Pelloski CE, Ballman KV, Furth AF, et al. Epidermal growth factor receptor variant III status defines clinically distinct subtypes of glioblastoma. J Clin Oncol 2007;25:2288–94.